



Synthesis and optoelectronic properties of new acceptor-donor-acceptor type solution processed conjugated small molecules for optoelectronics

Kakaraparthi Kranthiraja, Kumarasamy Gunasekar, Won-Tae Park, Yong-Young Noh & Sung-Ho Jin

To cite this article: Kakaraparthi Kranthiraja, Kumarasamy Gunasekar, Won-Tae Park, Yong-Young Noh & Sung-Ho Jin (2016) Synthesis and optoelectronic properties of new acceptor-donor-acceptor type solution processed conjugated small molecules for optoelectronics, Molecular Crystals and Liquid Crystals, 635:1, 57-66, DOI: [10.1080/15421406.2016.1200000](https://doi.org/10.1080/15421406.2016.1200000)

To link to this article: <http://dx.doi.org/10.1080/15421406.2016.1200000>



Published online: 01 Nov 2016.



Submit your article to this journal [↗](#)



Article views: 13



View related articles [↗](#)



View Crossmark data [↗](#)

Synthesis and optoelectronic properties of new acceptor-donor-acceptor type solution processed conjugated small molecules for optoelectronics

Kakaraparthi Kranthiraja^a, Kumarasamy Gunasekar^a, Won-Tae Park^b, Yong-Young Noh^b, and Sung-Ho Jin^a

^aDepartment of Chemistry Education, Graduate Department of Chemical Materials, Institute for Plastic Information and Energy Materials, Pusan National University, Busan, Republic of Korea; ^bDepartment of Energy and Materials Engineering, Dongguk University, Jung-gu, Seoul, South Korea

ABSTRACT



We designed and synthesized two new acceptor-donor-acceptor (A-D-A) small molecules SM-1 and SM-2 by connecting benzodithiophene (BDT) and dithienopyrrole (DTP) are electron rich donor units, dialkoxyphenylenedithiophene as π -spacer and 2,4 thiazolidinedione as terminal acceptor unit respectively. The SM-1 and SM-2 showed broad absorption windows with optical band gaps of 1.7 and 1.8 eV respectively, and also possess high thermal stabilities and suitable energy levels for optoelectronic applications. Especially, SM-2 shows a maximum power conversion efficiency of 1.26%, and hole mobility of $4.6 \times 10^{-3} \text{ cm}^2/\text{V.s}$ in conventional organic solar cells and organic field effect transistor devices respectively.

KEYWORDS

Benzodithiophene; dithienopyrrole; organic solar cell; organic field effect transistor

Introduction

Design and synthesis of versatile conjugated materials such as polymers and small molecules are becoming more fascinating for many research groups since they are the best encounters for inorganic silicon based materials with their unique features like light weight, low cost, flexibility and large area flexible fabrication [1]. Though the device performances of polymer based bulk heterojunction (BHJ) organic solar cells (OSCs) and field effect transistors (OFETs) and organic light emitting diodes (OLEDs) are high, purification of polymers, reproducibility are drawbacks for its commercial applications [2]. In this scenario, abilities like less variation for batch to batch, and high purity, no end-group contamination, driven small molecules into optoelectronic applications as potential alternative materials. However initial device performances of the small molecule based optoelectronics are low, upon additional attention on material design and device architectures could able to deliver high power conversion efficiencies (PCEs) in BHJ OSCs. Thus equal attention has been paying towards development of new small molecules to attain same or high device performances than polymer based devices [3].

CONTACT Sung-Ho Jin  shjin@pusan.ac.kr  Department of Chemistry Education, Graduate Department of Frontier Materials Chemistry, and Institute for Plastic Information and Energy Materials, Pusan National University, Busan 609-735, Korea. Color versions of one or more of the figures in the article can be found online at www.tandfonline.com/gmcl.

© 2016 Taylor & Francis Group, LLC

During last 10 years a rapid development happened in the design and synthesis of various kinds of small molecules where thiophene, selenophene, triphenylamine, benzodithiophene (BDT) are widely used as donor units, whereas benzothiadiazole, diketopyrrolopyrrole, and 2,4 thiazolidinedione or rhodanine were used as electron deficient acceptor units respectively and these donor and acceptor units were connected in various fashions such as donor-acceptor- donor (D-A-D), and acceptor-donor-acceptor (A-D-A) with π -spacer groups, and studied their optoelectronic properties and applied them into BHJ OSCs [3]. Among various design strategies A-D-A type small molecule design and synthesis has got best performance in BHJ OSCs [4]. In most of the cases bi-thiophene or terthiophene based π -spacers were used to connect donor and acceptor part to extend continuous conjugation and mobility but by implanting alkyl chain on to the thiophene based π -spacers may cause defects in planarity of backbone and cause adverse effects on device performances [5].

To address the above mentioned issues we have developed two small molecules with new π -spacer and connected them with two widely used donor molecules BDT, dithienopyrrole (DTP) and 2,4 thiazolidinedione dye type acceptor units. We believe that introduction of such spacers may induce additional planarity via interactions between oxygen atom of alkoxy side chain and sulfur atom of thiophene in π -spacer [6, 7]. Preliminary studies such as optoelectronic properties revealed that an enhanced vibronic shoulder was observed in the film state absorption spectra due to more aggregation; this phenomenon partly explains incorporation of the new spacer has some improved planarity of new small molecules up to certain extent. Further these small molecules were tested in BHJ OSCs and delivered PCE of maximum of 1.26% in conventional OSCs and which is well concurred with the maximum OFET hole mobility of SM-2 ($4.6 \times 10^{-3} \text{ cm}^2/\text{V.s.}$)

Experimental section

Materials and measurements

All chemicals and reagents were purchased from Sigma-Aldrich Chemical Co. Ltd, TCI, and Alfa Aesar, and were used without further purification. ^1H and ^{13}C NMR spectra were recorded on a Varian Mercury Plus 300 MHz spectrometer in CDCl_3 using tetramethylsilane (TMS) as an internal standard. The UV-vis absorption and the fluorescence spectra were recorded with a JASCO V-570 and Hitachi F-4500 fluorescence spectrophotometers at room temperature, respectively. Thermogravimetric analysis (TGA) and differential scanning calorimetry (DSC) thermogram were obtained with Mettler Toledo TGA/SDTA 851e and DSC 822e analyzer under an N_2 atmosphere at a heating rate of $10^\circ\text{C}/\text{min}$, respectively. ^1H and ^{13}C NMR spectra were recorded on a Varian Mercury Plus 300 MHz spectrometer in CDCl_3 using tetramethylsilane as an internal standard. Cyclic voltammetry (CV) measurements were carried out in a 0.1 M solution of tetrabutylammonium tetrafluoroborate in anhydrous chloroform at a scan rate of 100 mV/s using CHI 600C potentiostat (CH Instruments); three electrode cell with platinum electrode as the working electrode, Ag/AgCl as the reference electrode and a platinum (Pt) wire as the counter electrode were used. The highest occupied molecular orbital (HOMO) levels of the SM-1 and SM-2 were estimated from the CV, using the equation $\text{HOMO} = -(\text{E}_{\text{onset}}^{\text{ox}} - \text{ferrocene}_{\text{onset}}) - 4.8 \text{ eV}$, where E_{ox} is the onset oxidation potential relative to the ferrocene as standard material (0.38 V). The onset oxidation potential of SM-1 and SM-2 are 0.73 and 0.83 V. Further the lowest occupied molecular orbital (LUMO) energy levels were calculated from $\text{E}_{\text{g}}^{\text{opt}}$ and HOMO energy levels obtained from CV [8].

OFETs fabrication and characterization

Glass substrates (Corning Eagle XG) were cleaned sequentially in sonication baths of acetone, isopropanol, and deionized water for 10 minutes each. The device source/drain (S/D) electrode was patterned by conventional lift-off photolithography processes. Au and Cr (12 nm/2 nm) were used as source and drain metal electrodes. Semiconductors were prepared by dissolving new small molecules in anhydrous chloroform (5 mg / 1 mL) and the resulting solution was spin coated at 1500 rpm for 60 sec, and then thermally annealed at various temperatures such as 60, 100°C. Poly (methyl methacrylate) (PMMA) 80 mg /mL (Sigma Aldrich, ~ 120 kM_w) in n-Butyl acetate concentrate solution was spin coated at 2000 rpm for 60 sec and then baked at 80°C for 1 h in glove box (thickness ~ 500 nm, capacitance: 6.20 nF/cm²). The transistors were completed by depositing the top gate electrodes (Al) via thermal evaporation using a metal shadow mask. The electrical characteristics of the OFETs were extracted from the drain current via gate voltage bias or drain voltage bias (channel width (W)/length (L): 1000/20 μ m, respectively). All measurement was taken using Keithley 4200-SCs semiconductor parameter analyzer connected to glove box probe station.

Fabrication and characterization of the BHJ OSCs

The ITO and glass substrates that have been used for fabrication were ultrasonically cleaned with detergent, water, acetone, and isopropyl alcohol. Then, a 40 nm thick layer of PEDOT:PSS was coated on the electrodes by spin coating a solution of PEDOT:PSS diluted with isopropyl alcohol with the dilution ratio being 1:2 and annealed at 150°C for 10 min in oven. The active layer solutions were prepared with 1:1, 1:2, 1:3 donor: acceptor ratios in chloroform and stirred during overnight. The performances of the BHJ OSCs were measured under simulated AM 1.5G illumination (100 mW/cm²). The irradiance of the sunlight simulating illumination was calibrated using a standard Si photodiode detector fitted with a KG5 filter. The performance of the BHJ OSCs were measured using calibrated air mass (AM) 1.5G solar simulator (Oriel® Sol3A™ Class AAA solar simulator, models 94043A) with a light intensity of 100 mW/cm² adjusted using a standard PV reference cell (2 cm \times 2 cm monocrystalline silicon solar cell, calibrated at NREL, Colorado, USA) and a computer controlled Keithley 2400 source measure unit. The incident photon to current conversion efficiency spectrum was measured using Oriel® IQE-200™ equipped with a 250 W quartz tungsten halogen lamp as the light source and a monochromator, an optical chopper, a lock-in amplifier, and a calibrated silicon photodetector. The thickness of the thin films was measured using a KLA Tencor Alpha-step IQ surface profilometer with an accuracy of ± 1 nm. Atomic force microscopy (AFM) images were acquired with a XE-100 (park system corp.) in tapping mode.

Synthesis of SM-1

Intermediate 1 (0.3 g, 0.244 mmol), 2,4 thiazolidinedione (0.559 g, 2.44 mmol) were dissolved in chloroform (30 mL), and piperidine (0.1 mL) was added and refluxed for overnight. After completion of reaction, the reaction mixture was cooled to room temperature and extracted with chloroform, washed with brine solution and dried over anhydrous MgSO₄. The resulted crude was purified by column chromatography on silica gel with hexane: chloroform (5:5 v/v) to furnish red color solid. (Yield, 50%). ¹H NMR (300 MHz, CDCl₃): δ (ppm) 8.04 (m, 2H), 7.50–7.62 (m, 2H), 7.37 (m, 2H), 7.20–7.26 (m, 8H), 7.00 (m, 2H), 4.10–4.22 (m, 8H),

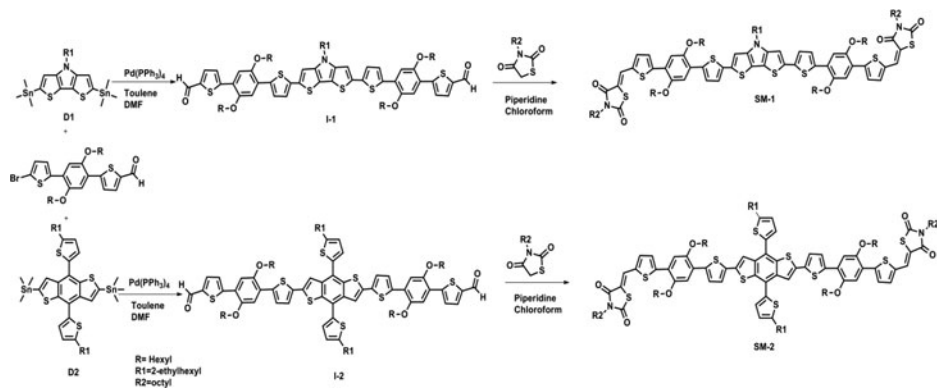
3.50–3.60 (m, 4H), 1.90–2.12 (m, 8H), 1.52–1.72 (m, 16H), 1.20–1.46 (m, 40H), 0.80–0.93 (m, 30H). ^{13}C NMR (75 MHz, CDCl_3): δ (ppm) 167.61, 166.14, 148.32, 146.44, 137.47, 133.38, 126.32, 126.57, 117.90, 111.30, 69.73, 51.12, 42.10, 40.33, 31.74, 29.44, 29.12, 29.08, 28.68, 27.79, 26.72, 28.17, 26.02, 24.08, 23.01, 22.64, 16.4, 12.4. MALDI-TOF: Calcd 1649.68. Found: 1649.86. Melting point (DSC): $\sim 190^\circ\text{C}$.

Synthesis of SM-2

Intermediate 2 (0.3 g, 0.19 mmol), 2,4 thiazolidinedione (0.45 g, 1.97 mmol) were dissolved in chloroform (30 mL), and piperidine (0.1 mL) was added and refluxed for overnight. Upon reaction completion, the reaction mixture was cooled to room temperature and extracted with chloroform, washed with brine solution and dried over anhydrous MgSO_4 . The resulted crude was purified by column chromatography on silica gel with hexane: chloroform (5:5 v/v) to furnish red color solid. (Yield, 52%). ^1H NMR (300 MHz, CDCl_3): δ (ppm) 8.05 (s, 2H), 7.69 (m, 2H), 7.58–7.60 (m, 2H), 7.53–7.54 (m, 2H), 7.37–7.39 (m, 2H), 7.34–7.35 (m, 2H), 7.22–7.28 (m, 6H), 6.94–6.95 (m, 2H), 4.10–4.16 (m, 8H), 3.71–3.76 (m, 4H), 2.89–2.91 (m, 4H), 1.91–2.03 (m, 8H), 1.62–1.64 (m, 10H), 1.34–1.47 (m, 56H), 0.85–1.00 (m, 30H). ^{13}C NMR (75 MHz CDCl_3): δ (ppm) 177.20, 166.22, 149.33, 145.92, 129.44, 128.32, 125.45, 119.30, 118.43, 114.09, 112.86, 106.18, 98.40, 93.80, 81.60, 69.77, 64.06, 58.59, 56.72, 55.11, 52.32, 43.36, 41.04, 34.34, 32.52, 31.75, 31.58, 29.15, 29.10, 28.95, 27.83, 26.74, 26.19, 25.97, 25.76, 23.09, 22.64, 14.10, 10.95. MALDI-TOF: Calcd 1938.95. Found: 1938.69. Melting point (DSC): $\sim 204^\circ\text{C}$.

Results and discussion

The synthetic routes for new conjugated small molecules SM-1 and SM-2 are shown in [scheme-1](#) and D1 and D2, and spacer were synthesized using already reported procedures [9, 10] and, intermediates 1 and 2 were synthesized via Stille coupling between D1 and D2 and spacer, and finally SM-1 and SM-2 were synthesized via Knoevenagel condensation between intermediates and 2,4 thiazolidinedione.



Scheme 1. Synthetic route for SM-1 and SM-2.

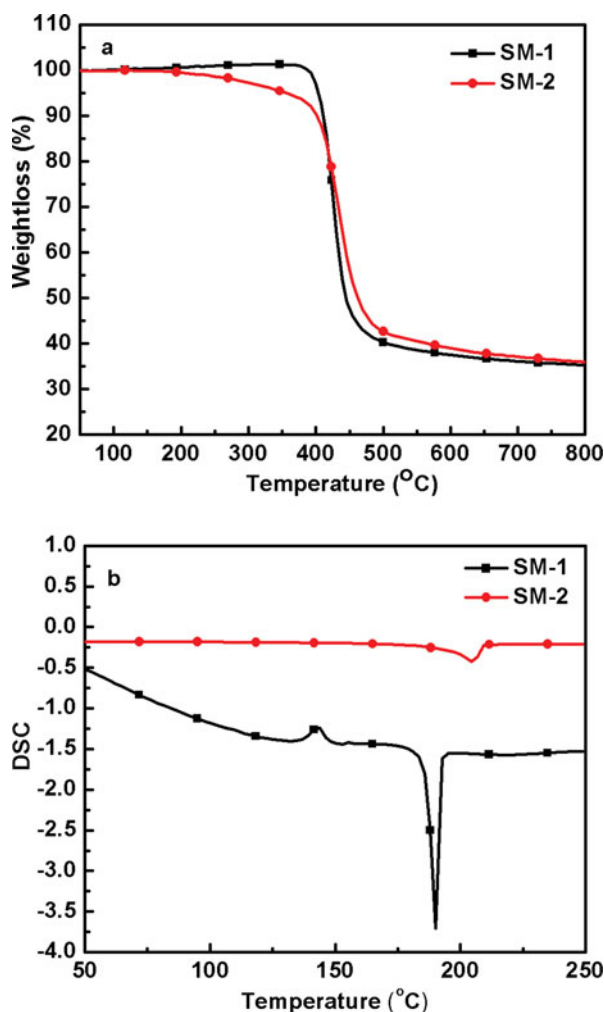


Figure 1. TGA, DSC profiles of SM-1 and SM-2.

Thermal properties

TGA and DSC were performed for SM-1 and SM-2 to study their thermal properties and the resulting TGA and DSC profile are shown in [Figure 1](#). The thermal decomposition temperatures of small molecules were found to be 362, 404°C and these high thermal stabilities are good enough for optoelectronic applications. The DSC profiles are SM-1 shows glass transition temperature (142°C) and melting temperature (~196°C), whereas SM2 shows only melting temperature at ~204°C.

Optical properties

UV-vis absorption spectra of SM-1 and SM-2 were measured in both solution and film state and spectra are displayed in [Figure 2](#) and data are shown [Table 1](#). Upon exchange of donor unit in small molecules, significant changes were observed in absorption spectra; especially SM-1 shows broad absorption windows in solution as well as in film state than SM-2. Bathochromic

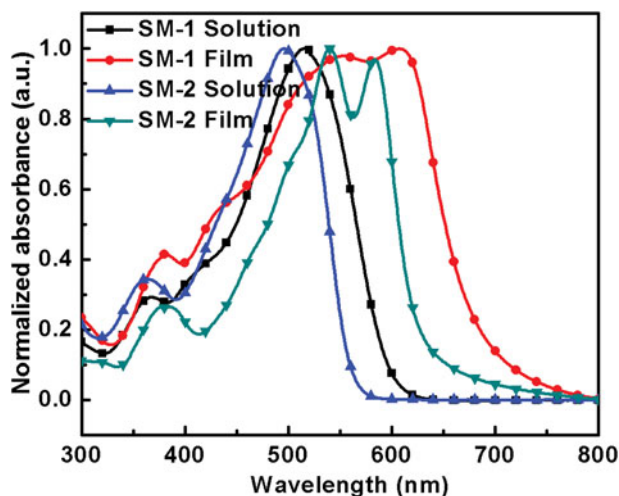


Figure 2. UV-vis absorption spectra of SM-1 and SM-2.

shifts in film state spectra for both the molecules were observed due to high aggregation and rigid co-planarization of new conjugated molecules. In film state the absorption maxima of SM-1 and SM-2 was red shifted (~ 90 nm) compared to that of solution counter parts. Additionally SM-1 and SM-2 shows vibronic shoulders in film state, and it is much pronounced in SM-2 than SM-1. The optical band gaps of small molecules are 1.7 and 1.8 eV respectively. Photoluminescence spectra of SM-1 and SM-2 are measured in chloroform solution, and the emission range of SM-1 and SM-2 are 550–800 nm and 515–750 nm. An emission maximum of SM-1 was 60 nm red shifted than SM-2 and the emission maxima of SM-1 and SM-2 are 643 and 583 nm, respectively.

Electrochemical properties

In order to investigate the electrochemical properties of SM-1 and SM-2, CV studies were performed to estimate their HOMO and LUMO energy levels. The resulting cyclic voltammograms of the SM-1 and SM-2 are shown [Figure 3](#). The onset oxidation potentials of SM-1 and SM-2 are 0.73, 0.83 V respectively. The calculated HOMO energy levels are -5.15 and -5.25 eV and the LUMO levels are found to be -3.45 eV which can provide enough LUMO level offset between the SM-1, SM-2 and PC₆₁BM for good exciton dissociation at the donor acceptor interface.

Table 1. Optical and electrochemical properties of SM-1 and SM-2.

Material	Solution λ_{\max} [nm] ^a	Film λ_{\max} [nm] ^b	Film λ_{\max} [nm] ^c	E_g^{opt} [eV] ^d	HOMO [eV]	LUMO [eV] ^e
SM-1	514	550, 607	729	1.70	-5.15	-3.45
SM-2	489	532, 576	688	1.80	-5.25	-3.45

^aAbsorption maxima measured from UV-vis absorption spectrum in chloroform.

^bAbsorption maxima measured from UV-vis absorption spectrum in thin film state.

^cThe onset of the film absorption edge.

^dEstimated from the onset of the absorption in thin films ($E_g^{\text{opt}} = 1240/\lambda_{\text{onset}}$)

^eCalculated from the difference of HOMO and optical band gap.

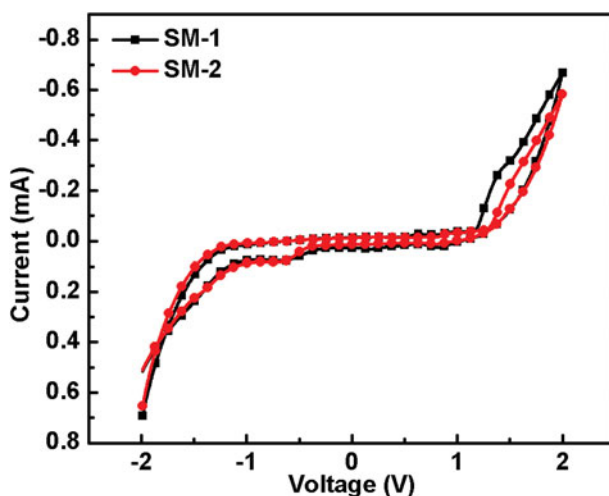


Figure 3. Cyclic voltammetry of SM-1 and SM-2.

OFETs properties

OFETs were fabricated with new small molecules in top gate, bottom contact geometry with a PMMA gate dielectric layer. The new small molecules displayed prominent field effect hole mobilities indicates they possess p-type behavior and resulting transfer characteristics and OFET mobilities are shown in Figure 4 and Table 2. In order to improve the field effect mobilities we have baked the transistors at various temperatures 60 and 100°C. Both SM-1 and SM-2 showed improvement in mobilities upon increasing the baking temperature from 60 to 100°C.

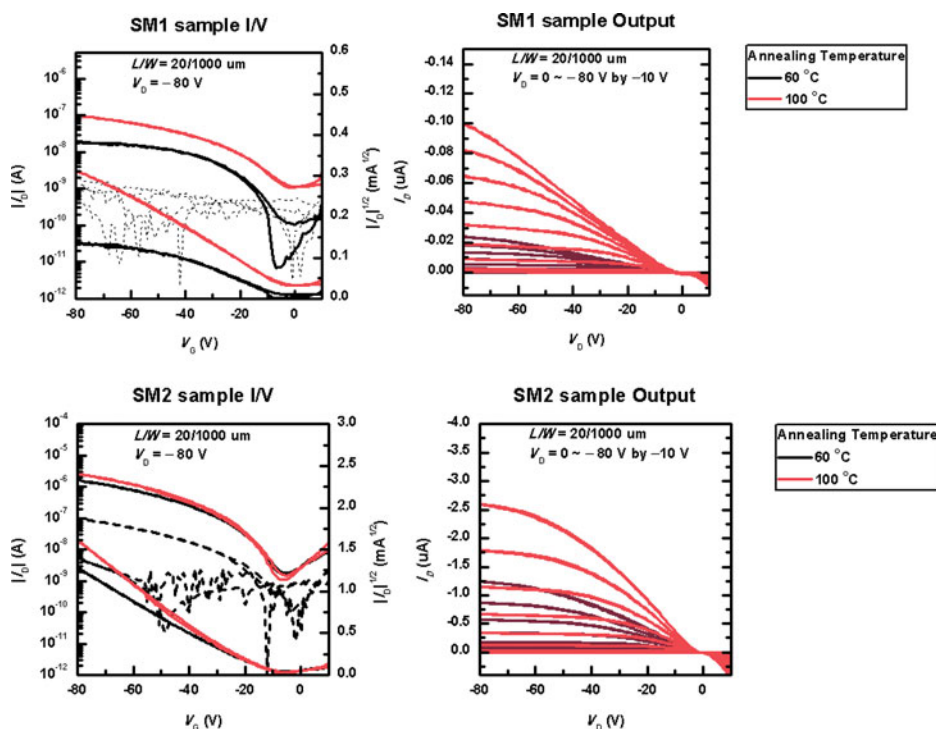


Figure 4. Transfer and output characteristics of OFETs based on SM-1 and SM-2.

Table 2. Transfer characteristics of SM-1 and SM-2.

Material	Annealing temperature (°C)	μ sat cm ² /V.s	V _{TH} (V)	S.S (V/dec.)
SM-1	60	5.2×10^{-5}	− 4.13	− 2.41
SM-1	100	1.2×10^{-4}	0.93	− 17.14
SM-2	60	2.6×10^{-4}	− 16.73	− 9.96
SM-2	100	4.6×10^{-3}	− 19.89	− 6.69

The OFET mobilities of SM-1 are 5.2×10^{-5} and 1.2×10^{-4} cm²/V.s respectively. And SM-2 displayed 2.6×10^{-3} and 4.6×10^{-3} cm²/V.s at 60 and 100°C respectively, from the obtained results we can expect SM-2 based BHJ OSCs can show good photovoltaic parameters.

Photovoltaic properties

In order to find out the photovoltaic properties of new conjugated small molecules, BHJ OSCs were fabricated with conventional device structure of ITO/PEDOT:PSS/SM-1 and SM-2:PC₆₁BM/LiF/Al. The active layers were spin coated from different solvents and chloroform was found to be the best solvent for these two new conjugated small molecules. We have tried various blending ratios from 1:1–1:3 to get best photovoltaic performance for new small molecules since blending ratio can significantly impact on active layer morphology. The optimized donor and acceptor ratio for SM-1 and SM-2 1:3 and 1:2 respectively. The optimized photovoltaic properties of SM-1 and SM-2 are 0.15 and 0.93%. The lower PCEs of SM-1 based devices are due to low open-circuit voltage (V_{oc}), fill factor (FF), short-circuit current density (J_{sc}), whereas higher PCE of SM-2 is attributed to its high J_{sc}, FF, and V_{oc} and also high hole mobility. Since the V_{oc} of OSCs depends on difference between HOMO of donor (SM-1 and SM-2) and LUMO of acceptor (PC₆₁BM), the higher V_{oc} values of SM-2 than SM-1 could be attributed to the deeper HOMO energy level of SM-2. Further higher J_{sc} of SM-2 based OSCs might be due to the broad absorption spectra, relatively favorable active layer morphology and higher OFET hole mobility. The current density - voltage (J-V) curves of devices are shown in Figure 5, and the resulting photovoltaic properties of the all compositions are shown in Table 3.

It is known that improvement of photovoltaic properties of BHJ OSCs is possible by various techniques such as thermal annealing, addition of external additives and solvent vapor annealing. Among them post thermal annealing is widely applied and most successful technique in the small molecules based OSCs, which results in enhanced PCE in case of SM-2 based devices. To improve the photovoltaic properties we have tried various post thermal annealing temperatures such as 80, 100, 120°C, in which at 80°C there is notable improvement in PCE up to 1.26% for SM-2 based devices, and it could be due to the improved nanoscale morphology of active layer, which would have improved the J_{sc}, FF and V_{oc}, and the obtained PCE is well concurred with the OFET mobility results.

Morphology

The surface topography of optimized active layer blends SM-1: PC₆₁BM (1:3) and SM-2: PC₆₁BM (1:2-thermal annealing at 80°C) were recorded by AFM operated in tapping mode, to understand the morphological properties, since morphology is very important factor to be studied in BHJ OSCs. The root mean square (RMS) roughness of the optimized blend active layers of SM-1: PC₆₁BM (1:3) and SM-2: PC₆₁BM (1:2-thermal annealing) are found to be 4.3

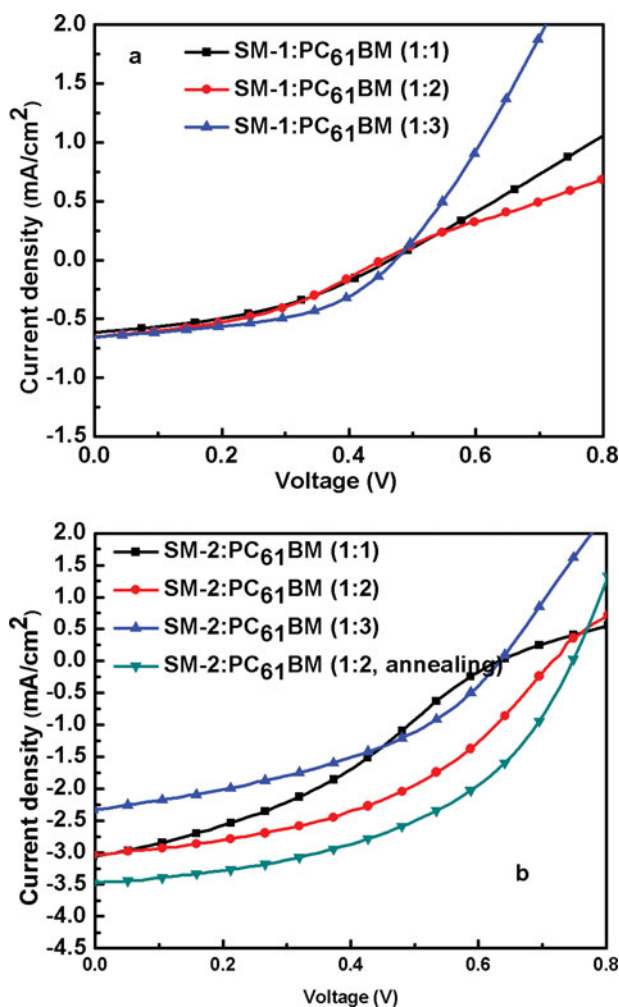


Figure 5. J-V Characteristics of optimized devices of SM-1 and SM-2.

and 3.3 nm respectively as shown in Figure 6. Even though both the films shows crystalline domains and aggregates, there could be a possibility of insufficient phase separation and poor charge transport in blends leads to poor device performance of small molecules, when compared to two new synthesized molecules based OSCs, SM-2: PC₆₁BM (1:2-thermal annealing) based blend possess comparatively better phase separation compared to the SM-1: PC₆₁BM (1:3) which is well correlated with its photovoltaic properties.

Table 3. Optimized photovoltaic properties of SM-1 and SM-2 based OSCs.

Small Molecule	Ratio	V_{oc}	J_{sc}	FF	PCE
SM-1	1:1	0.46	0.64	0.40	0.11
SM-1	1:2	0.48	0.56	0.45	0.12
SM-1	1:3	0.47	0.64	0.48	0.15
SM-2	1:1	0.67	2.99	0.34	0.69
SM-2	1:2	0.71	3.03	0.45	0.93
SM-2	1:3	0.65	2.03	0.38	0.60
SM-2	1:2 ^a	0.74	3.46	0.48	1.26

^aThermal annealing at 80°C.

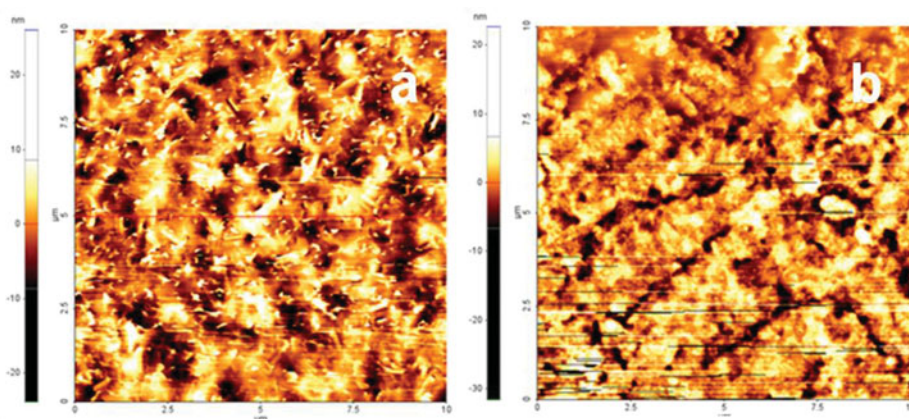


Figure 6. AFM images of SM-1:PC₆₁BM (1:3) and SM-2: PC₆₁BM (1:2-thermal annealing at 80°C).

Conclusions

In summary we synthesized two new A-D-A type conjugated small molecules SM-1 and SM-2 with new π -spacer for optoelectronic applications, both SM-1 and SM-2 showed good optoelectronic properties such as broad absorption profiles, suitable HOMO and LUMO energy levels and good thermal properties. BHJ OSCs of SM-2 could able to deliver maximum PCE of 1.26%, and moderately high OFET hole mobility of $4.6 \times 10^{-3} \text{ cm}^2/\text{V.s}$ clearly explains the role of new spacers in enhancing the planarity of small molecules. Further fine tuning of structure of SM-1 and SM-2 have possibility of improving the PCE further along with suitable device optimization techniques.

Acknowledgments

This work was supported by a grant from the National Research Foundation of Korea (NRF) of the Ministry of Science, ICT & Future Planning (MSIP) of Korea (NRF-2011-0028320) and the Pioneer Research Center Program through the National Research Foundation of Korea funded by the Ministry of Science, ICT & Future Planning (MSIP) of Korea (NRF-2013M3C1A3065522).

References

- [1] Cheng, Y.-L., Yang, S.-H., & Hsu, C.-S. (2009). *Chem. Rev.*, 109, 5868.
- [2] Cinar, M.-E., & Ozturk, T. (2015). *Chem. Rev.*, 115, 3036.
- [3] Chen, Y., Wan, X., & Long, G. (2013). *Acc. Chem. Res.*, 46, 2645.
- [4] Liu, Y., Chen, C.-C., Hong, Z., Gao, J., Yang, Y., Zhou, H., Dou, L., Li, G., & Yang, Y. (2013). *Sci. Rep.*, 3, 3356.
- [5] Lan, S.-C., Chang, C.-K., Lu, Y.-H., Lin, S.-W., Jen, A.-K.-Y., & Wei, K.-H. (2015). *RSC Adv.*, 5, 67718.
- [6] Kranthiraja, K., Gunasekar, K., Cho, W., Song, M., Park, Y.-G., Lee, J.-Y., Shin, Y., Kang, I.-N., Kim, A., Kim, H., Kim, B., & Jin, S.-H. (2014). *Macromolecules*, 47, 7060.
- [7] Kranthiraja, K., Gunasekar, K., Chakravarthi, N., Song, M., Moon, J.-H., Lee, J.-Y., Kang, I.-N., & Jin, S.-H. (2015). *Dyes and Pigm.*, 123, 100.
- [8] Cheon, Y.-R., Kim, Y.-J., Ha, J.-J., Kim, M.-J., Park, C.-E., & Kim, Y.-H. (2014). *Macromolecules*, 47, 8570.
- [9] Li, Y. (2012). *Acc. Chem. Res.*, 45, 723.
- [10] Geng, Y., Dai, H., Chang, S., Hu, F., Zeng, Q., & Wang, C. (2015). *ACS Appl. Mater. Interfaces*, 7, 4659.